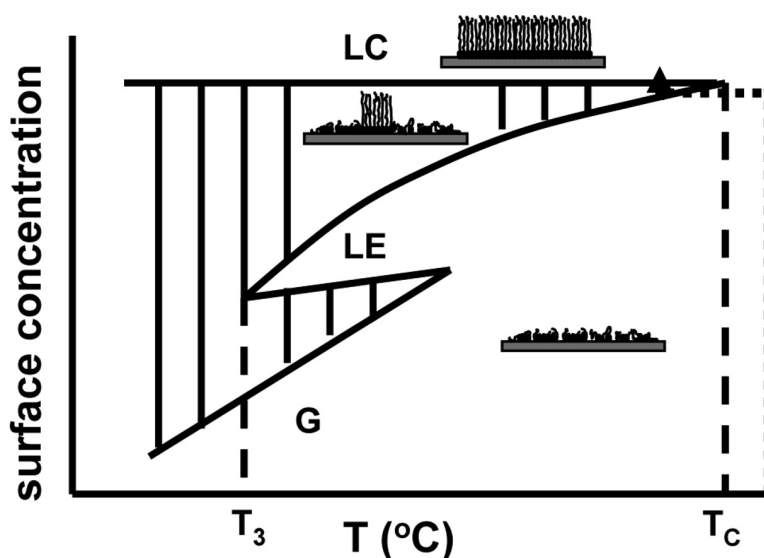


## Supercritical Self-Assembled Monolayer Growth

James M. Mellott, and Daniel K. Schwartz

*J. Am. Chem. Soc.*, **2004**, 126 (30), 9369-9373 • DOI: 10.1021/ja0489588 • Publication Date (Web): 13 July 2004

Downloaded from <http://pubs.acs.org> on April 1, 2009



### More About This Article

Additional resources and features associated with this article are available within the HTML version:

- Supporting Information
- Links to the 1 articles that cite this article, as of the time of this article download
- Access to high resolution figures
- Links to articles and content related to this article
- Copyright permission to reproduce figures and/or text from this article

[View the Full Text HTML](#)

## Supercritical Self-Assembled Monolayer Growth

James M. Mellott<sup>†,‡</sup> and Daniel K. Schwartz<sup>\*‡</sup>

Contribution from the Department of Chemistry, Tulane University,  
New Orleans, Louisiana 70118, and Department of Chemical and Biological Engineering,  
University of Colorado, Boulder, Colorado 80309

Received February 24, 2004; E-mail: daniel.schwartz@colorado.edu

**Abstract:** The growth of octadecyltrimethylammonium bromide (C<sub>18</sub>TAB) monolayers on mica was investigated using atomic force microscopy and infrared spectroscopy. A critical temperature was identified below which the monolayer formed via an "islanding" mechanism, that is, nucleation and growth of densely packed two-dimensional (2D) islands within a matrix of a disordered dilute phase. However, above the critical temperature, there was no coexistence of 2D phases during film formation. Instead, the monolayer gradually became better ordered, remaining laterally homogeneous throughout. We show that this corresponds to a critical point in a 2D phase diagram of the monolayer. Additional evidence is provided by the in situ observation of 2D phase separation upon cooling an incomplete monolayer from the one-phase to the two-phase region. The lack of coexisting domains (and domain boundaries) during growth above the critical point provides a possible route for the preparation of essentially defect-free monolayers.

## Introduction

Molecular self-assembly is generally recognized as a powerful biomimetic strategy for the fabrication of nanoscale structures. Among purely synthetic systems, self-assembled monolayers (SAMs) are the prototypical example of two-dimensional molecular organization. The defining characteristic of molecular self-assembly is that molecular interactions lead spontaneously to a well-organized equilibrium structure. Generally, these interactions are "soft" and reversible, because adjustment and molecular motion are necessary to minimize defects and achieve organized assemblies. Thus, by necessity, self-assembly is highly dynamic; that is, it is unlikely that one can design a self-organizing system that is simultaneously well-organized and rigid/static. This suggests that the rational design of stable nanoscale structures requires a complete understanding of the equilibrium structure and phase behavior of molecular assemblies.

A number of recent observations<sup>1–5</sup> suggest that it is useful to consider the structure of incomplete SAMs, for example, during the growth process, within the context of a 2D phase diagram.<sup>6</sup> In other words, although the entire three-dimensional system (monolayer and solution) is not in full equilibrium until the chemical potential of a molecule within the film is equal to that of a molecule in solution, the instantaneous structure of

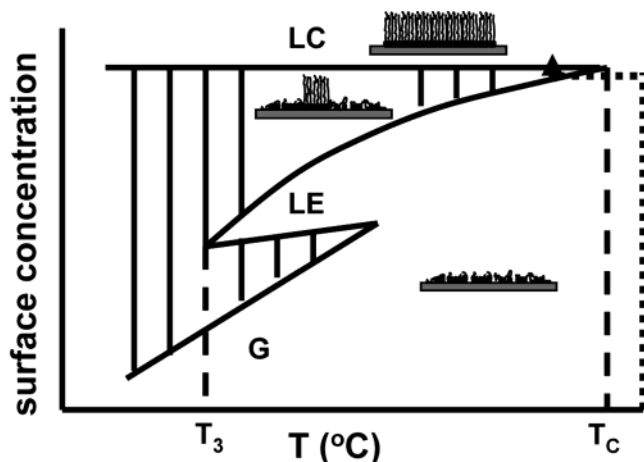
the adsorbed monolayer during growth attempts to minimize a 2D free energy. If molecular transport within the layer permits rearrangement on time scales short as compared to the adsorption rate, then the structure during growth approximates one consistent with an isothermal path through a 2D phase diagram. Even if surface rearrangement is relatively slow, the existence of an underlying equilibrium phase diagram can provide insight into qualitative SAM growth mechanisms. For example, the coexistence of various 2D phases has been identified during the growth of various SAM systems;<sup>1–5,7–9</sup> a mechanistic change analogous to a triple point has also been observed.<sup>1</sup> Alkyltri-alkoxysilanes and alkyltrichlorosilanes have been observed to adsorb on silicon into different phases dependent on the deposition temperature.<sup>3,5</sup> Carraro et al. also observed the adsorption of a liquid condensed phase above a transition temperature.<sup>3</sup> Messerschmidt and Schwartz have reported the observation of growth of a solid 2D phase from either a liquid or a gaseous phase for octadecylphosphonic acid on sapphire depending on the temperature of deposition.<sup>1</sup>

Figure 1 depicts a schematic 2D phase diagram, the low-temperature portion of which ( $T < T_C$ ) is proposed to describe the coexistence of two phases during the growth of a SAM. This phase diagram is composed of three different phases: the gaseous (G) highly disordered and dilute phase, the liquid expanded (LE) phase which is more dense although still disordered (the continuous phase observed at lower temperatures in this work), and the liquid condensed (LC) phase which is a densely packed and highly ordered phase (the LC phase corresponds to the islands observed at lower temperatures). Messerschmidt and Schwartz have shown evidence of the triple

<sup>†</sup> Tulane University.<sup>‡</sup> University of Colorado.

- (1) Schwartz, D. K.; Messerschmidt, C. *Langmuir* **2001**, *17*, 462–467.
- (2) Goldmann, M.; Davidovits, J. V.; Silberzan, P. *Thin Solid Films* **1998**, *329*, 166–171.
- (3) Carraro, C.; Yauw, O. W.; Sung, M. M.; Maboudian, R. *J. Phys. Chem. B* **1998**, *102*, 4441–4445.
- (4) Sung, M. M.; Carraro, C.; Yauw, O. W.; Kim, Y.; Maboudian, R. *J. Phys. Chem. B* **2000**, *104*, 1556–1559.
- (5) Parikh, A. N.; Allara, D. L.; Azouz, I. B.; Rondelez, F. *J. Phys. Chem.* **1994**, *98*, 7577–7590.
- (6) Schwartz, D. K. *Annu. Rev. Phys. Chem.* **2001**, *52*, 107.

(7) Hayes, W. A.; Schwartz, D. K. *Langmuir* **1998**, *14*, 5913.(8) Poirier, G. E. *Langmuir* **1999**, *15*, 1167–1175.(9) Taylor, C. E.; Schwartz, D. K. *Langmuir* **2003**, *19*, 2665–2672.



**Figure 1.** Quasi-equilibrium phase diagram consistent with the observation of a solid–liquid critical point. The dotted line represents the approximate path of the temperature ramp experiment through the phase diagram.

point ( $T_3$ ) with the use of AFM on ex situ samples.<sup>1</sup> In Figure 1, the critical point ( $T_C$ ) is the hypothetical temperature above which only supercritical growth occurs.

If such a phase diagram model of SAM growth were valid, one would expect to observe critical behavior at high temperatures. In this scenario, above a critical temperature, SAM growth would no longer involve coexistence of 2D phases, and the replacement of a less dense phase by nucleation and growth of islands of a more dense phase. Instead, the growth of the SAM would proceed by gradual densification and organization of a laterally homogeneous supercritical 2D fluid. In this article, we report the first direct observation of such a phenomenon. This could have important practical implications because the absence of coexisting domains during growth results in a final film devoid of grain boundary defects.

## Experimental Section

Octadecyltrimethylammonium bromide ( $C_{18}$ TAB) (99% purity) and hexadecane (99% purity) were purchased from Aldrich (Aldrich, Milwaukee, WI) and used as received. Water from a Milli-Q UV+ purification system (Millipore, Bedford, MA) was used for the preparation of the 0.10 mM  $C_{18}$ TAB/ $H_2O$  solution. High-grade mica was purchased from Ted Pella, Inc. (Redding, CA).

For in situ AFM experiments, a Nanoscope III AFM-E was used in contact mode, and the temperature was controlled using a custom-made temperature stage placed on top of the piezoelectric scanner tube. The temperature stage was identical to the one described by Schwartz and Sikes,<sup>10</sup> and it was controlled by an Omega PID temperature controller (model # CN77353, Omega Engineering, Inc, Stanford, CT). The temperature stage was composed of a Peltier element (model # FCO.65-31-04-1L, Melcor Corp., Trenton, NJ) sandwiched between two copper disks 0.46 mm thick. A Type-K thermocouple (Omega Engineering, Inc., Stanford, CT) was used to measure the temperature of the stage and was sandwiched between the Peltier element and the top copper disk and immobilized with thermally conductive epoxy. An aluminum nitride epoxy (Melcor Corp., Trenton, NJ) was used to construct the stage. The mica sample was attached to the temperature stage using conductive carbon tabs purchased from Ted Pella, Inc. The temperature stage was calibrated by inserting a type K thermocouple inside the liquid cell full of water and collecting a series of data points through the temperature range of interest. A linear fit of the data was made to determine the temperature at the water–mica interface.

The liquid cell provided by Digital Instruments was used as received, and for in situ experiments etched-silicon cantilevers ( $k = 0.7$ – $1.4$  N/m, NanoDevices) were used in contact mode. These cantilevers were chosen because during heating they expand uniformly, whereas Au-coated silicon nitride cantilevers act as a bimetallic strip and curl as the temperature changes. Before each in situ experiment, the liquid cell was rinsed in absolute ethanol and dried with a dry nitrogen stream. The liquid cell was then placed in a Boekel UV-cleaner for 5 min to further ensure there were no remnant organic molecules in the system. For all experiments, the substrate was allowed to stabilize at the setpoint temperature with Millipore water in the liquid cell for 30 min before 0.10 mM  $C_{18}$ TAB solution was introduced.

To study the adsorption above 50 °C directly, two different types of in situ AFM experiments were performed. The first was a “temperature step” experiment in which a solution of 0.10 mM  $C_{18}$ TAB/ $H_2O$  was introduced into the liquid cell (containing a mica substrate) held at 60 °C. The mica was left in contact with solution for 1–1.5 h without imaging. After this period of time, several AFM images were captured to verify that the adsorbed layer was featureless. Next, the temperature stage was turned off, allowing the liquid cell to reach the ambient system temperature of 32.4 °C, and the system was left undisturbed for an additional 67 min. After this time, the AFM was re-engaged, and force curves and height images were captured.

The second type of in situ experiment performed was the “temperature ramp” which was a slow real-time temperature ramp where the AFM tip remained in contact and imaging while the temperature of the fluid cell was decreased from 51.9 to 45.4 °C. The initial steps in this experiment were the same as those of the “temperature step” experiment where 0.10 mM  $C_{18}$ TAB/ $H_2O$  was introduced into the liquid cell at 51.9 °C and the temperature was maintained for 1 h without imaging. After 1 h, a force curve and AFM image were captured to verify that a bilayer was present on the surface and that the surface was uniformly flat. An AFM scan was then started with a scan rate of 1.42 Hz and a scan size of  $30 \times 30 \mu\text{m}^2$ . These parameters allowed for the temperature to be lowered at the rate of 1 °C/1 min/5  $\mu\text{m}$ . The AFM tip was kept in contact with the surface during this process. Thus, the temperature decreased during the scan, and the vertical axis of the scan indicates both the position on the sample as well as the temperature. It was possible to follow the surface structure in real time as the temperature was decreased from 51.9 to 45.4 °C. When the scan was finished, another scan was taken of the same area of the surface, but the temperature of the cell was kept at a constant 45.4 °C.

For ex situ experiments, the samples were prepared by immersing freshly cleaved 12.5 cm mica disks into solutions thermostated at 53 °C for the specified time. Upon removal from solution, the samples were rinsed with Millipore water to remove excess solution and then blown dry with dry nitrogen. The ex situ samples were characterized using AFM and FTIR. The AFM characterization was performed with either a Nanoscope III MMAFM or an AFM-E (Digital Instruments, Santa Barbara, CA). All ex situ AFM images were collected in contact mode with silicon nitride tips ( $k = 0.12$  N/m). (At least three regions per sample were imaged.) Several samples at each specific immersion time were imaged. Coverage information was measured using a histogram of the height profile of each image with the Nanoscope software.

Transmission narrow band infrared spectra were obtained using a Thermo Nicolet Nexus 470 FTIR spectrometer. The FTIR was equipped with a narrow band MCT/A detector with an incident IR beam of 6.4 mm (defined by the sample holder). Due to the low signal level, IR data were averaged over 2400 scans (at 2  $\text{cm}^{-1}$  resolution) for the sample and then ratioed to a 2400 scan background to enhance the signal-to-noise ratio. For a background sample, the original sample was placed in a Boekel UV-cleaner for 30 min to remove the monolayer. The spectra were subsequently filtered with an FFT and notch filter in IgorPro v.4.0 (Wavemetrics, Inc., Lake Oswego, OR) to remove the

(10) Schwartz, D. K.; Sikes, H. D. *Science* **1997**, *278*, 1604–1607.

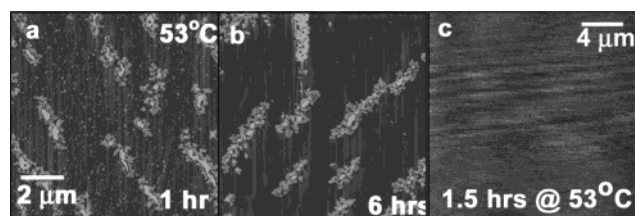


**Figure 2.** (a and b) Representative ex situ AFM images of SAMs prepared at 53 °C and quenched after the immersion time annotated. The higher features represent remnants of a disordered bilayer as shown previously.<sup>11</sup> There is no evidence of increased coverage of higher features with increased immersion. The low (monolayer) regions are featureless. (c) Representative in situ AFM image at 53 °C. Such images are featureless and do not exhibit the bilayer patches observed on ex situ samples.

interference pattern caused by the mica, and a boxcar filter was then used to smooth the data.

## Results

The growth process of C<sub>18</sub>TAB self-assembled monolayers on mica between 22 and 50 °C involves the initial adsorption of a liquid expanded (LE) phase that is quickly shielded from the aqueous solution by a second (inverted) layer. Islands of a liquid condensed (LC) phase nucleate with a very low activation barrier and grow to cover the surface. The maximum density of the LE phase was observed to increase with temperature. These results were reported previously in greater detail.<sup>11</sup>

Above 53 °C, however, in situ and ex situ AFM images, supported by ex situ IR observations, suggest that monolayer growth is not accompanied by the nucleation and growth of LC islands. Figure 2a and b is representative of ex situ AFM images at 53 °C quenched after different immersion times, and Figure 2c is a representative in situ AFM image at 53 °C after 1.5 h in contact with solution. No topographical or lateral force (friction) features are evident in Figure 2c, consistent with a laterally homogeneous surface. The images of quenched films (Figure 2a and b) do show features of various size and shape. However, the height of these features (~2 nm), the comparison with in situ images, and the fact that the fractional coverage of the features does not depend on immersion time (remaining at ~10%) suggests that they represent remnants of a second layer (described in greater detail in previous work<sup>11</sup>), stable in solution, that is not completely detached during the removal of the SAM from solution. Thus, the lower areas surrounding these patches are, in fact, the continuous molecular monolayer. In marked contrast with incomplete SAMs formed below 50 °C, no islands are present within the monolayer regions. To summarize, in situ and ex situ AFM images of incomplete SAMs at 53 °C do not vary substantially as a function of immersion time. In all cases, they are consistent with the presence of a laterally homogeneous monolayer.

Nevertheless, FTIR spectra of quenched samples (Figure 3) show that the average molecular order within the film increases continuously with immersion time. Figure 3 is a plot of the asymmetric methylene peak position versus immersion time. The blue shift in Figure 3 indicates increasing molecular order from essentially liquidlike molecules (2924 cm<sup>-1</sup>) to all-trans crystalline alkyl chains (2918 cm<sup>-1</sup>).<sup>7,12,13</sup> Given the fact that

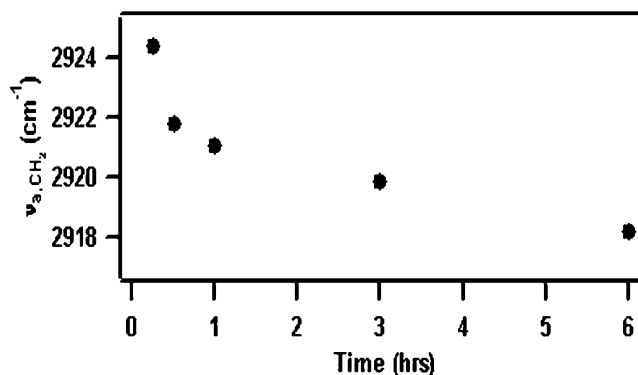


**Figure 3.** Plot of the asymmetric methylene stretching frequency versus immersion time for ex situ samples at 53 °C.

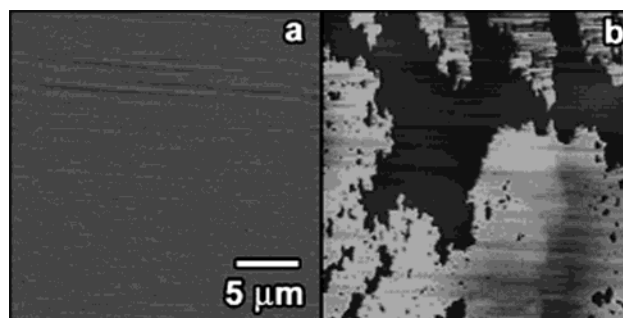


**Figure 4.** In situ AFM images from the temperature step experiment. (a) AFM image of the surface at 51.9 °C after 90 min in 0.10 mM C<sub>18</sub>TAB. (b) The same region after 67 min at 32.5 °C.

the coverage of bilayer patches does not increase with immersion time, we conclude that the molecular order gradually increases within the monolayer phase, which appears laterally homogeneous in the AFM images. This is consistent with supercritical behavior.

To study the adsorption above 50 °C directly, two different types of in situ AFM experiments were performed: “temperature step” and “temperature ramp”. Figures 4a and b show representative AFM images of the “temperature step” experiment. Figure 4a is a 25 × 25 μm<sup>2</sup> height mode image at 60 °C that is featureless, indicating a one-phase film. As shown below, the force curves captured during these experiments indicate the presence of a bilayer.<sup>11,14–17</sup> Figure 4b is a representative image of the surface after the temperature was decreased to 32.4 °C; in this image, the large islands are consistent with the coexistence of LE and LC phases of C<sub>18</sub>TAB on mica. After phase separation was observed, the fluid cell was heated to 60 °C and left without imaging for 1–2 h. After this waiting period, the coexisting phases were still present, suggesting the phase separation was not reversible on these time scales.

Force curves provide direct evidence that an adsorbed film is, in fact, present under the high-temperature conditions where AFM images show a uniform surface (e.g., Figure 4a). Figure 5a shows the force curve of the approach between a Si<sub>3</sub>N<sub>4</sub> AFM tip and bare mica in pure water. It demonstrates the expected hard repulsive contact between the tip and the substrate, without

(11) Mellott, J. M.; Schwartz, D. K.; Hayes, W. A. *Langmuir* **2004**, *20*, 2341–2348.

(12) Lin-Vein, D.; Colthup, N. B.; Fateley, W. G.; Grasselli, J. G. *The Handbook of Infrared and Raman Characteristic Frequencies of Organic Molecules*; Academic Press: San Diego, 1991.

(13) Woodward, J. T.; Doudevski, I.; Sikes, H. D.; Schwartz, D. K. *J. Phys. Chem. B* **1997**, *101*, 7535.

(14) Israelachvili, J. N. *Intermolecular and Surface Forces*, 2nd ed.; Academic Press: London, 1991.

(15) Ducker, W. A.; Liu, J. *J. Phys. Chem. B* **1999**, *103*, 8558.

(16) Ducker, W. A.; Wanless, E. J. *Langmuir* **1999**, *15*, 160.

(17) Ducker, W. A.; Liu, J.; Min, G. *Langmuir* **2001**, *17*, 4895.



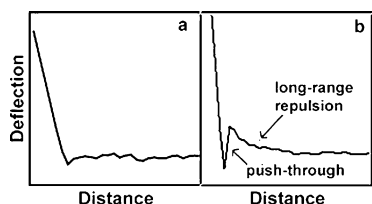


**Figure 5.** (a) A representative force curve between the AFM tip and mica in water. (b) A representative force curve obtained in 0.10 mM  $C_{18}TAB$  solution at 60 °C.

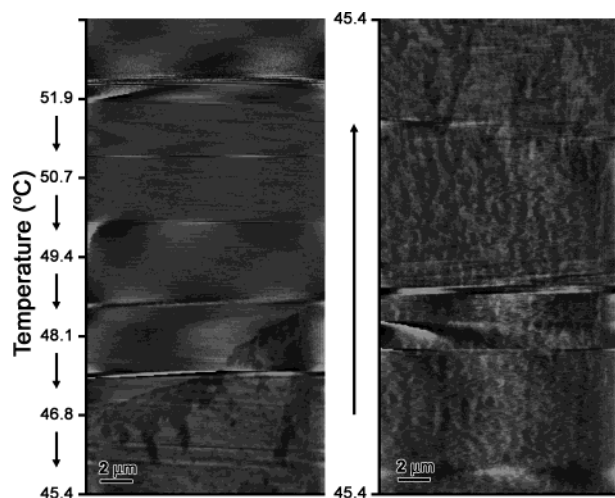


**Figure 6.** Lateral force AFM images during a “temperature ramp” experiment. The slow scan direction of the left image is down, and for the right image the scan direction is up as indicated by the arrows. The left image shows the phase separation occurring between 49.4 and 48.1 °C. The right image is a scan of the same region as the left image after the temperature reached 45.4 °C, demonstrating that the whole surface has phase-separated.

evidence of long-range repulsion or adhesion. In contrast, Figure 5b is a force curve for the approach between a Si AFM tip and mica in 0.10 mM  $C_{18}TAB$  at 60 °C. The upward curve in Figure 5b is a result of a long-range repulsive electrical double layer<sup>14</sup> force between the AFM tip and the surface — this feature has been previously interpreted as evidence of bilayer or micellar structures in alkylammonium systems.<sup>11,15–17</sup> Upon closer approach, the tip is observed to push through the adsorbed layer.

The second type of in situ experiment performed was a gradual real-time temperature ramp where the AFM tip remained in contact and imaging while the temperature of the fluid cell was decreased from 51.9 to 45.4 °C. Figure 6 shows representative AFM images of the “temperature ramp” experiment. On the left side of Figure 6, between 51.9 and 49.4 °C the surface appears featureless as in Figure 4a. Between 49.4 and 48.1 °C, however, two regions with different frictional responses were observed on the surface, and as the temperature was ramped the rest of the way to 45.4 °C the lower friction region was observed to cover more of the surface and the two phases were in coexistence. The entire right image of Figure 6, obtained immediately following the temperature ramp, shows the coexistence of the two different phases, suggesting that the surfactants have phase-separated on the entire surface. Lateral force images are shown because the height differences between phases are very small near the transition, as would be expected in the vicinity of a critical point. In fact, our previous work<sup>11</sup> showed that the height difference of coexisting phases during growth decreased as the temperature increased toward 50 °C.

## Discussion

The results presented above suggest a distinct change in the  $C_{18}TAB$  SAM growth mechanism at ~50 °C. Below this temperature,  $C_{18}TAB$  on mica adsorbs first into an LE phase that densifies until it reaches a maximum concentration<sup>11</sup> at which point LC phase islands nucleate and grow. Thus, monolayer growth at lower temperature involves the coexistence of two 2D phases. Above 50 °C, however, several observations indicate that growth proceeds via gradual ordering within a single laterally homogeneous phase. In particular, the monolayer portion of AFM images of quenched SAMs is always laterally homogeneous; that is, no islands were observed in the lower areas. Similarly, in situ AFM images above 50 °C show homogeneous films, with no islands present, regardless of immersion time. However, FTIR data show a gradual ordering of alkyl chains with immersion time. The most likely conclusion that reconciles these observations is that the tailgroups within the laterally homogeneous film gradually become better ordered to the point where they are vibrationally indistinguishable from all-trans crystalline alkyl chains. Within the scenario presented earlier, where SAM growth is considered within the context of an isothermal path through a 2D phase diagram, the results presented here indicate the presence of a critical point at ~50 °C.

In situ temperature ramp experiments corroborate these observations by directly demonstrating phase separation of LE and LC phases when an incomplete, but laterally homogeneous, supercritical SAM is cooled from above 50 °C to below 50 °C. The approximate thermodynamic path taken in these in situ experiments is indicated in Figure 1 by the dotted line showing the gradual increase in density of a homogeneous supercritical 2D liquid (during the isothermal incubation period), followed by a decrease in temperature into the LE–LC coexistence region. Of course, the increase in density during supercritical growth cannot be observed by AFM, but is inferred from FTIR measurements. We propose that these observations are consistent with an LE–LC critical point ( $T_c$ ), extending the analogy previously proposed between SAMs and Langmuir monolayers.<sup>1,3,5</sup> Furthermore, this interpretation is also consistent with our previous observation<sup>11</sup> that the height difference between coexisting phases decreases as the critical point is approached from below, that is, the coexistence region narrows.

A recent report of a 2D melting transition in this system<sup>18</sup> is probably a distinct phenomenon from that observed here. In those experiments, a completely formed SAM was heated ex situ, and chain melting was observed at ~60 °C.

## Conclusions

The LE–LC critical point for the growth of octadecyltrimethylammonium bromide self-assembled monolayers was determined using a combination of AFM and FTIR on quenched SAMs and by the use of temperature-controlled in situ AFM experiments. Quasi-equilibrium phase diagrams similar to Langmuir phase diagrams have been used to provide insight into SAM growth mechanisms in many different systems, and in this case we propose a phase diagram in which growth between 22 and ~50 °C is multistep with adsorption into a liquid expanded layer and then growth of liquid condensed islands

(18) Osman, M. A.; Seyfang, G.; Suter, U. W. *J. Phys. Chem. B* **2000**, *104*, 4433–4439.

from within this liquid layer. Above a critical temperature of  $\sim 50$  °C, however, SAM growth occurs by gradual densification and ordering of a laterally homogeneous supercritical 2D phase. The lack of coexisting domains (and domain boundaries) during growth above the critical point provides a possible route for the preparation of essentially defect-free monolayers.

**Acknowledgment.** J.M.M. thanks the Louisiana Board of Regents Louisiana Education Quality Support Fund for a fellowship. This work was supported by the National Science Foundation (Award No. CHE-0349547).

JA0489588